Water Supply

IWA PUBLISHING

Water Supply Vol 22 No 5, 4822 doi: 10.2166/ws.2022.190

Insights into the enhanced fluoranthene degradation in citric acid coupled Fe(II)-activated sodium persulfate system

Jiaqi Dong, Xianxian Sheng, Yulong Liu, Peng Wang, Zhanpeng Lu, Qian Sui and Shuguang Lyu *

State Environmental Protection Key Laboratory of Environmental Risk Assessment and Control on Chemical Process, East China University of Science and Technology, Shanghai 200237, China
*Corresponding author. E-mail: lvshuguang@ecust.edu.cn

ABSTRACT

Polycyclic aromatic hydrocarbons (PAHs), which are present in contaminated groundwater, have attracted increasing attention because of their serious harm to humans. In this study, the degradation performance of fluoranthene (FLT), a typical tetracyclic PAHs in organic contaminated sites, was investigated in the persulfate (PS)/Fe(II)/citric acid (CA) system. The effects of PS, CA, and Fe(II) doses on FLT degradation were tested. With the molar ratio at 60/20/5/1 of PS/Fe(II)/CA/FLT, FLT removal reached 96.3% in 120 min, much higher than 62% removal without CA at the same PS and Fe(II) doses, indicating that the addition of CA could remarkably enhance the FLT degradation. The water quality conditions (pH, anions and humic acid) were also investigated for their effects on FLT degradation. The results of probe tests, electron paramagnetic resonance detection and scavenging experiments showed that $HO^{\bullet}$ and $SO_4^{-\bullet}$ acted predominantly on FLT degradation. The influence of surfactants on FLT degradation was examined. Furthermore, the primary degradation intermediates of FLT were detected by GC-MS and the possible degradation pathways of FLT were proposed. Finally, the effectiveness of the PS/Fe(II)/CA process for the FLT degradation in actual groundwater demonstrated that the process has a great prospect for the remediation of FLT-contaminated groundwater.

Key words: chelated-Fe(II) activation, citric acid (CA), fluoranthene (FLT), groundwater remediation, persulfate (PS)

HIGHLIGHTS

- The enhancing effect of CA on FLT degradation was investigated.
- $HO^{\bullet}$ and $SO_4^{-\bullet}$ were the primary ROS in the PS/Fe(II)/CA system for FLT degradation.
- The possible degradation pathways of FLT were proposed.
- The effects of surfactants on FLT degradation were investigated.
- Effective degradation of FLT in actual groundwater was achieved.

GRAPHICAL ABSTRACT

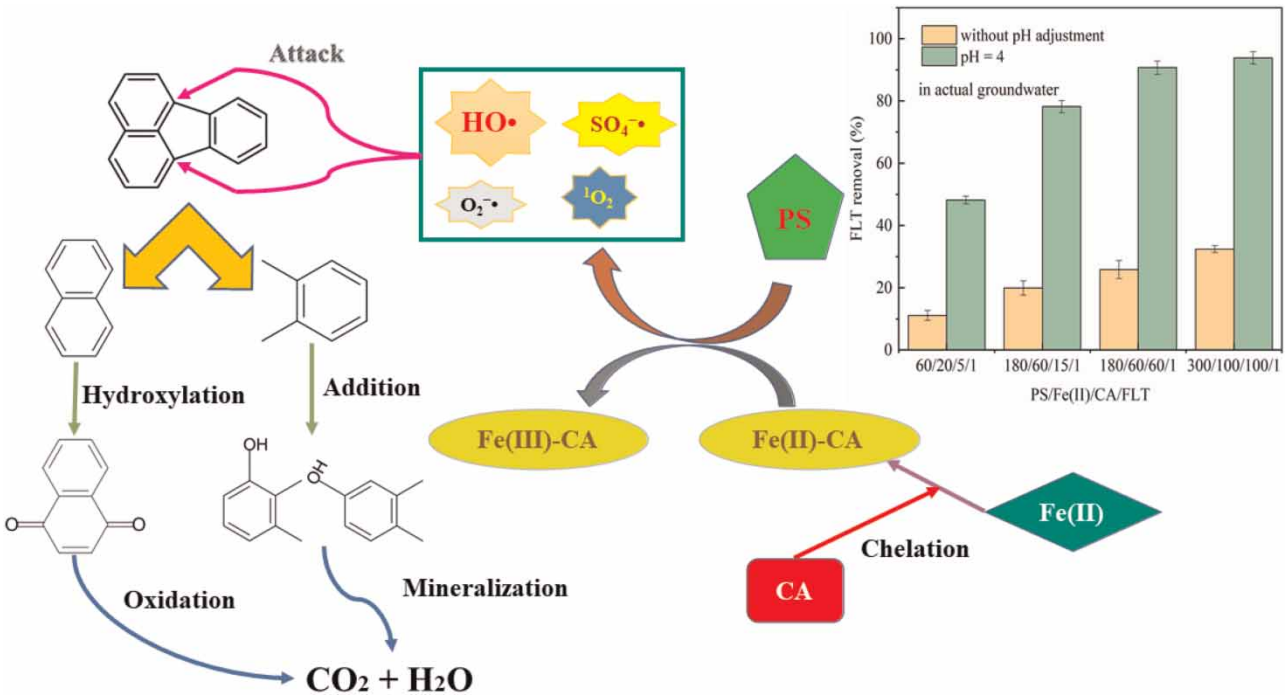

1. INTRODUCTION

Polycyclic aromatic hydrocarbons (PAHs), which are a class of hazardous organic chemicals with two or more benzene rings, are widely present in the environment due to the incomplete combustion of coal, fuel and wood (Keyte *et al.* 2013). Fluoranthene (FLT), one of the typical tetracyclic PAHs with carcinogenic property and difficult degradation (Kadri *et al.* 2017), is on the priority list of PAHs regulated by the U.S. Environmental Protection Agency (USEPA) due to its high content and frequent detection in various countries, including China (Wang *et al.* 2017). Therefore, the elimination of PAHs, including FLT, from contaminated soil and groundwater has become an urgent task, and the corresponding technologies are diversely developed.

In recent years, *in situ* chemical oxidation (ISCO) has played an increasingly important role in the remediation of organics contaminated soil and groundwater (Baciocchi 2013; Qian *et al.* 2016). In Fenton and Fenton-like processes, oxidants including percarbonate (SPC), persulfate (PS), potassium permanganate and hydrogen peroxide (H_2O_2) (Ghauch *et al.* 2011) are commonly used to generate reactive oxygen species (ROS), which are essential for pollutant degradation. In particular, PS, which combines the advantages of H_2O_2 and other oxidants, is becoming more and more popular in ISCO (Lindsey & Tarr 2000). PS not only has strong stability but also produces $HO^{\bullet}$ and $SO_4^{-\bullet}$ by chain reactions after activation (Lindsey & Tarr 2000), which can destruct hard-to-degrade pollutants, including PAHs (Peluffo *et al.* 2016). There are various activation methods for PS, such as thermal activation (Ghauch *et al.* 2015), UV activation (Ghauch *et al.* 2017), alkali activation and transition metals activation, among them transition metals activation is highly appreciated for its cost-effective and simple operating condition (Wang & Wang 2018). This activation method includes not only plated zero valent iron (ZVI), but also bimetallics (Ghauch *et al.* 2013), trimetallics (Ayoub & Ghauch 2014) or even iron scrap (Naim & Ghauch 2016). Compared with other transition metals, Fe-based catalysts (Fe(II), Fe(III), Fe0, MOFs, etc.) are commonly employed for their inexpensive, high-efficiency and environmentally friendly features (Rastogi *et al.* 2009a; El Asmar *et al.* 2021). The reaction stoichiometric efficiency (RSE) is the number of moles of probes degraded over the number of moles of PS consumed (Baalbaki *et al.* 2018; Tantawi *et al.* 2019). Generally, the % RSE values can vary a lot in different systems. For example, PS activated with iron powder showed % RSE around 5% while if Fe is used in MOF systems, the % RSE reached 30–40%, and the thermal activation showed an even greater value up to 70% and UV_{254} activation reached 55% (Table 1). They also correlated the % RSE with the total organic carbon (TOC) removed (Ghauch *et al.* 2017). Fe(II), as

Table 1 | Comparison of % RSE in different systems for pollutant removal

Catalytic systems	RSE (%)	pollutant	Reaction time (min)	References
Fe_0/PS	5.2	Sulfamethoxazole	120	Ghauch *et al.* (2013)
Fe/Cu/PS	11	2,4-dichlorophenol	60	Fang *et al.* (2021)
iFe/PS	72	Ranitidine	60	Naim & Ghauch (2016)
MIL-88-A/PS	19.7–33.45	Naproxen	120	Asmar *et al.* (2021)
UV_{254}/PS	52	Chloramphenicol	60	Ghauch *et al.* (2017)
Thermal/PS	7.5–68	Naproxen	90	Ghauch *et al.* (2015)
Fe(II)/CA/PS	2.9	Fluoranthene	120	present work

one of the transition metal ions, can catalyze PS to produce $SO_4^{-\bullet}$ that degrades the target pollutant (Equation (1)):

$$S_2O_8^{2-} + Fe(II) \rightarrow Fe(III) + SO_4^{2-} + SO_4^{-\bullet} \quad (1)$$

However, it also has been found that Fe(II) can consume $HO^{\bullet}$ and $SO_4^{-\bullet}$ when it is in excess (Equations (2) and (3)). In addition, when the pH of the solution is greater than 4, Fe(II) and Fe(III) are prone to form precipitates, causing a decrease in the concentration of dissolved iron ions (Gupta & Gupta 1981). Some researchers tried to overcome these drawbacks and boosted the removal of contaminants by adding chelating agents such as citric acid (CA) and ethylene diamine tetraacetic acid (EDTA) (Liang *et al.* 2004, 2009; Wu *et al.* 2014). Zhang *et al.* (2017) found that the CA addition could enhance the activation of PS by nano zero-valent iron (nZVI) effectively, thus promoting the 2,4,6-trichloroanisole degradation. Yan & Lo (2013) also discovered that ethylenediamine-N, N′-disuccinic acid (EDDS) and EDTA could enhance the PS/Fe(II) process to some extent. CA, a natural organic acid that is widely found in nature, is extensively used in environmental remediation because of its excellent chelating ability, biodegradability and environmental friendliness (Wu *et al.* 2014). So far, little research has been reported on PS oxidation for FLT degradation that is enhanced by Fe(II) coupled with CA. Further confirmation of the reaction mechanisms for FLT degradation in the PS/Fe(II)/CA system is still needed, and the possible degradation pathways of FLT need to be revealed. Further, the surfactants are frequently used as a pretreatment step in soil remediation due to their effective desorption effect to PAHs in contaminated soil. So it is also necessary to explore the effect of surfactants on this process.

$$Fe(II) + HO^{\bullet} \rightarrow Fe(III) + HO^{-} \quad (2)$$

$$Fe(II) + SO_4^{-\bullet} \rightarrow Fe(III) + SO_4^{2-} \quad (3)$$

Therefore, the objectives of this study are to: (1) investigate the efficiency of FLT removal in PS/Fe(II)/CA system and study the effect of dose of chemicals on FLT removal; (2) explore the effect of groundwater matrices on FLT degradation in the PS/Fe(II)/CA system; (3) identify the primary ROS for the FLT degradation in the PS/Fe(II)/CA system and propose possible degradation pathways for FLT by analyzing the intermediates produced in the PS/Fe(II)/CA system; (4) reveal the effect of surfactants on FLT degradation; and (5) evaluate the effectiveness of the PS/Fe(II)/CA system for FLT removal in actual contaminated groundwater.

2. MATERIALS AND METHODS

2.1. Regents and chemicals

The details of materials used in this study are available in the Supplementary material.

2.2. Experimental procedures

The FLT stock solution (0.004 M) was prepared by employing 0.0202 g solid FLT with 25 mL acetone and then stored in the refrigerator at 4 °C. All FLT degradation experiments were conducted in a 250 mL cylindrical glass reactor (an inner diameter

of 6.0 cm and a height of 9.0 cm) with two openings on the top for dosing and sampling in which a magnetic stirrer (600 r min^{-1}) was used to keep the homogeneity of the aqueous solution. The temperature in all batch reactions was controlled at 20 ± 0.5 °C by a low-temperature water bath (DC, Ningbo, China) and the initial solution pH was unadjusted. According to the EPA DSSTox database, FLT has a relative molecular mass of 202.25 and a solubility of 0.20–0.26 mg L^{-1} in.water. The FLT concentration was set at 0.001 mM which corresponds to the concentration of FLT at actual PAHs-contaminated groundwater (Ogbuagu *et al.* 2011). 0.001 mM of FLT was prepared by adding 0.25 mL of FLT stock solution to a volumetric flask containing 1 L ultrapure water (groundwater used for actual groundwater tests) for dissolution for 8–10 hr. The addition of acetone was so small that it could not affect the reaction. First, the FLT solution was transferred into the reactor. Second, the predetermined amounts of $FeSO_4 \cdot 7H_2O$ and CA were added to the solution successively. After Fe(II) and CA were mixed homogeneously, a designed dosage of PS was added to initiate the reaction. At the predetermined time, 0.5 mL samples were taken out to a 5 mL vial pre-filled with 0.5 mL methanol to terminate the reaction. Afterwards, the samples were filtered by 0.22 μm millipore membrane for high-performance liquid chromatography (HPLC) analysis. To investigate the influence of the initial pH of the solution, the initial solution pH was adjusted by 0.10 M NaOH or 0.10 M H_2SO_4, otherwise, the initial solution pH was unadjusted.

For the experiments concerning the influence of groundwater matrixes, sodium bicarbonate, sodium chloride or humic acid was initially added into the reactor containing FLT, then other chemicals were added later as in the FLT experiments. The remaining content of FLT was determined by HPLC at the predetermined time. In the experiment exploring the effect of surfactants on FLT degradation, the surfactant was added first and other reagents were added later, then the FLT concentration was analyzed by HPLC at the predetermined reaction time. All tests were conducted at least in triplicate and the mean values were reported.

2.3. Analytical methods

The concentration of FLT was analyzed by HPLC (LC-20AT, Shimadzu, Japan) at the detection wavelength of 235 nm. The mobile phase was a mixture of ultrapure water and methanol (10:90 (v/v)). The oven temperature was 30 °C and the injection value was 100 μL.

The intermediates during FLT degradation were analyzed by GC-MS (Agilent, G2577A, USA) equipped with a flame ionization detector (FID) and an HP-5MS capillary column (Li *et al.* 2019a, 2019b). Electron paramagnetic resonance (EPR) tests for active radical analyses were conducted on a Bruker EMX-8/2.7C spectrometer using DMPO or TEMP as spin-trapping compound. The instrumental conditions are described in the Supplementary material.

The residual PS concentration was monitored using the KI colorimetric method (Liang *et al.* 2008). The concentrations of Fe(II) and total Fe in the aqueous solution were determined by *o*-phenanthroline spectrophotometry (Harvey *et al.* 1955). The explicit analytical methods used in this work are shown in the Supplementary material.

3. RESULTS AND DISCUSSION

3.1. Comparison of FLT degradation in various systems

Figure 1 shows FLT degradation in different systems, among which the molar ratio of PS/Fe(II)/CA/FLT is 60/20/5/1. In the blank test, it can be seen that up to 4.7% FLT was lost in the solution, indicating that the volatilization of FLT was well controlled in the entire experiment. FLT degradations of 6.4 and 13.6% were achieved when only Fe(II) or PS along were added, indicating no direct reaction of Fe(II) with FLT when compared with the blank result, and the PS reaction with FLT in aqueous solution was also generally slow. For the PS/Fe(II) system, FLT was degraded rapidly in the initial 5 min (50% removal), then more than 12% was removed in the next 105 min. This two-stage degradation process was also observed in another report (Gan & Ng 2012) and it could be inferred that a large number of ROS were generated immediately with enough PS and available Fe(II) initially, but concurrently leading to massive consumption of Fe(II) and larger accumulation of Fe(III) in the following time, therefore losing the activation function. It is noteworthy that FLT degradation was increased dramatically from 62 to 96.3% in 120 min reaction after adding CA into the PS/Fe(II) system. Compared with the PS/Fe(II) system, the PS/Fe(II)/CA system had a persistent degradation of FLT in the whole reaction time, proving the significant effectiveness of CA in the PS oxidative process on FLT degradation. There may be several reasons for the enhancement of the FLT degradation by CA. On the one hand, the pH of the solution was decreased from 5.34 to 4.82 (Table 2) after adding CA, which could prevent the precipitation of irons and hold the soluble iron in the solution to a certain extent. On the other hand,

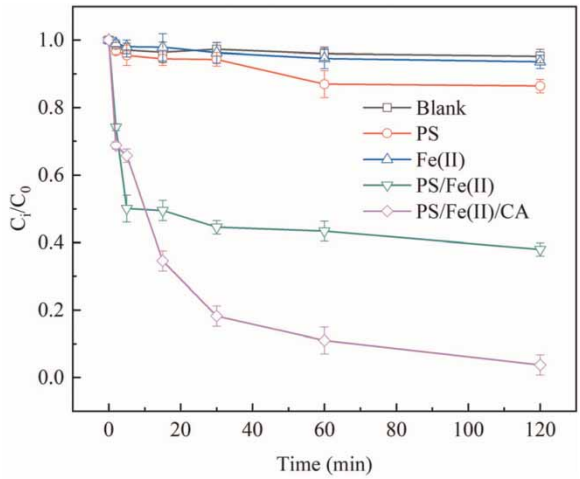

Figure 1 | FLT degradation performance in various systems. $[PS]_0 = 0.06$ mM, $[Fe\ (II)]_0 = 0.02$ mM, $[CA]_0 = 0.005$ mM, $[FLT]_0 = 0.001$ mM.

Table 2 | Parameter values in PS/Fe(II)/CA system

Experimental conditions PS/Fe(II)/CA/FLT	pH (initial/final)	FLT removal (%)
60/20/0/1	5.34/4.06	62.0
60/20/5/1	4.82/3.92	96.3
*60/20/5/1	8.07/7.92	11.1
*pH = 4	3.98/4.06	48.2
*180/60/15/1	8.01/7.95	20.0
*pH = 4	4.00/3.83	78.2
*180/60/60/1	7.91/7.81	25.9
*pH = 4	4.03/3.91	90.7
*300/100/100/1	7.31/7.12	32.5
*pH = 4	4.05/3.63	93.9

*Experiments were conducted by using the actual groundwater.

CA may elevate iron solubility by forming Fe(II)/Fe(III)-CA complexes, and promote Fe(II) recycling by altering the redox conditions (Liang *et al.* 2004).

In order to determine whether the improvement of FLT removal was due to the effect of pH reduction or the effect of Fe(II)/Fe(III)-CA complexes, the initial solution pH of the PS/Fe(II) process was adjusted to 4.82 which was in line with the unadjusted pH of the PS/Fe(II)/CA system. Although the initial pH dropped to 4.82 in the PS/Fe(II) system, FLT removal was only 6.2% higher than the unadjusted one (Figure 2). In addition, the soluble Fe and oxidant concentrations during the reaction were determined. As illustrated in Figure S1b, the total Fe in the PS/Fe(II) system was significantly lower than that in the PS/Fe(II)/CA system, which confirmed that CA could increase the concentration of soluble iron by forming Fe(II)/Fe(III)-CA complexes. Besides, the PS consumption increased with the addition of CA, which implied the generation of more ROS, thus enhancing FLT degradation.

3.2. Effect of chemical dosages on FLT degradation

To further explore the degradation performance of FLT in the PS/Fe(II)/CA system, the effect of chemical dosages was investigated. First, the experiments were performed by keeping the dosages of Fe(II) and CA at 0.02 and 0.005 mM, respectively, while the dosage of PS was changed from 0.02 to 0.12 mM to investigate the effect of PS dosage on FLT degradation. As shown in Figure 3(a), FLT degradation was improved significantly with the increase of PS concentration from 0.02 to 0.06 mM, which demonstrated that more ROS would be generated with the appropriate enhancement of PS concentration.

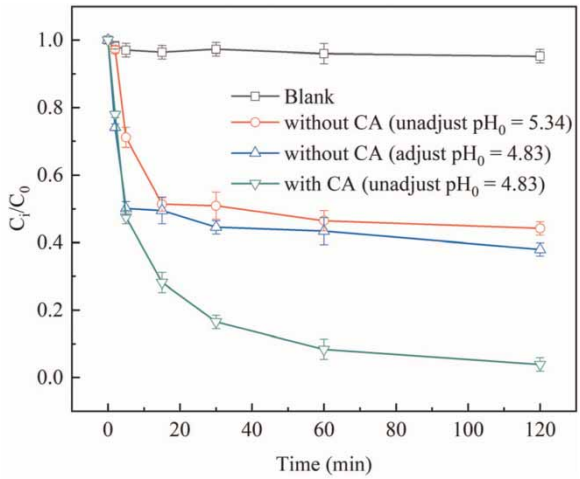

Figure 2 | Effect of pH change caused by CA on FLT degradation. $[PS]_0 = 0.06$ mM, $[Fe\ (II)]_0 = 0.02$ mM, $[CA]_0 = 0.005$ mM, $[FLT]_0 = 0.001$ mM.

Nevertheless, when the dosage of PS further increased to 0.12 mM, FLT removal had barely changed. This phenomenon may be due to the fact that the $SO_4^{-\bullet}$ concentration increased with the PS concentration and the excess $SO_4^{-\bullet}$ could react with $S_2O_8^{2-}$, $SO_4^{-\bullet}$ and $HO^{\bullet}$, leading to some unnecessary loss of ROS (Equations (4)–(6)):

$$SO_4^{-\bullet} + S_2O_8^{2-} \rightarrow SO_4^{2-} + S_2O_8^{-\bullet} \quad (4)$$

$$SO_4^{-\bullet} + SO_4^{-\bullet} \rightarrow S_2O_8^{2-} \quad (5)$$

$$SO_4^{-\bullet} + HO^{\bullet} \rightarrow HSO_4^{-} + 1/2O_2 \quad (6)$$

Despite the fast reaction in the first 2 min, FLT degradation in the PS/Fe(II)/CA system within 2–60 min was in accordance with the pseudo-first-order reaction kinetic model (Equations (7)–(9)). As illustrated in Figure S2a and Table S3, the calculated rate constants (k) significantly increased from 0.0062 ($R^2 > 0.67$) to 0.0326 min^{-1} ($R^2 > 0.92$) when PS dosage was increased from 0.02 to 0.06 mM, and the FLT removal half-time ($t_{1/2}$) was decreased from 111.8 to 21.3 min. However, upon increasing the PS dose from 0.06 to 0.12 mM, k showed a slight decrease along with a minor increase in $t_{1/2}$, which indicated that k would not increase and t would not decrease indefinitely with increasing PS concentration. Therefore, considering the FLT removal and avoiding waste, the PS dosage was set at 0.06 mM in the following experiments:

$$dC_i/dt = -k \times C_i \quad (7)$$

$$\ln(C_i/C_0) = -kt \quad (8)$$

$$t_{1/2} = \ln 2/k \quad (9)$$

Second, the amount of Fe(II) was varied to study the effect of Fe(II) on FLT degradation, and the amounts of PS and CA were controlled at 0.06 and 0.005 mM, respectively, and the results are shown in Figure 3(b), Figure S2b and Table S3. As the Fe(II) concentration rose from 0.005 to 0.02 mM, FLT degradation and k were increased from 73.5 to 96.3% and from 0.0105 to 0.0326 min^{-1}, and $t_{1/2}$ was reduced from 66.0 to 21.3 min, respectively. However, the adverse phenomenon of FLT degradation, k and $t_{1/2}$ were observed when the Fe(II) concentration increased to 0.04 and 0.06 mM. FLT removal decreased by 5.6 and 11.5%, k reduced to 0.0308 and 0.0227 min^{-1}, and $t_{1/2}$ increased to 22.5 and 30.5 min, respectively, indicating that excess Fe(II) would in turn deplete the ROS in solution (Rastogi *et al.* 2009a).

Finally, further investigation was conducted to explore the effect of CA dosage on FLT removal. In the experiment, the doses of PS and Fe(II) were 0.06 and 0.02 mM, respectively. The consequences, which are presented in Figure 3(c), Figure S2c and Table S3, are similar to the effects of PS and Fe(II) doses on FLT degradation as described above. When CA was set as 0.02 mM, although FLT degradation was almost unchanged, k was significantly lower than that of 0.005 and 0.01 mM CA, and $t_{1/2}$ was the opposite. This was mainly owing to the following two reasons. For one thing, ROS would react with CA causing unnecessary

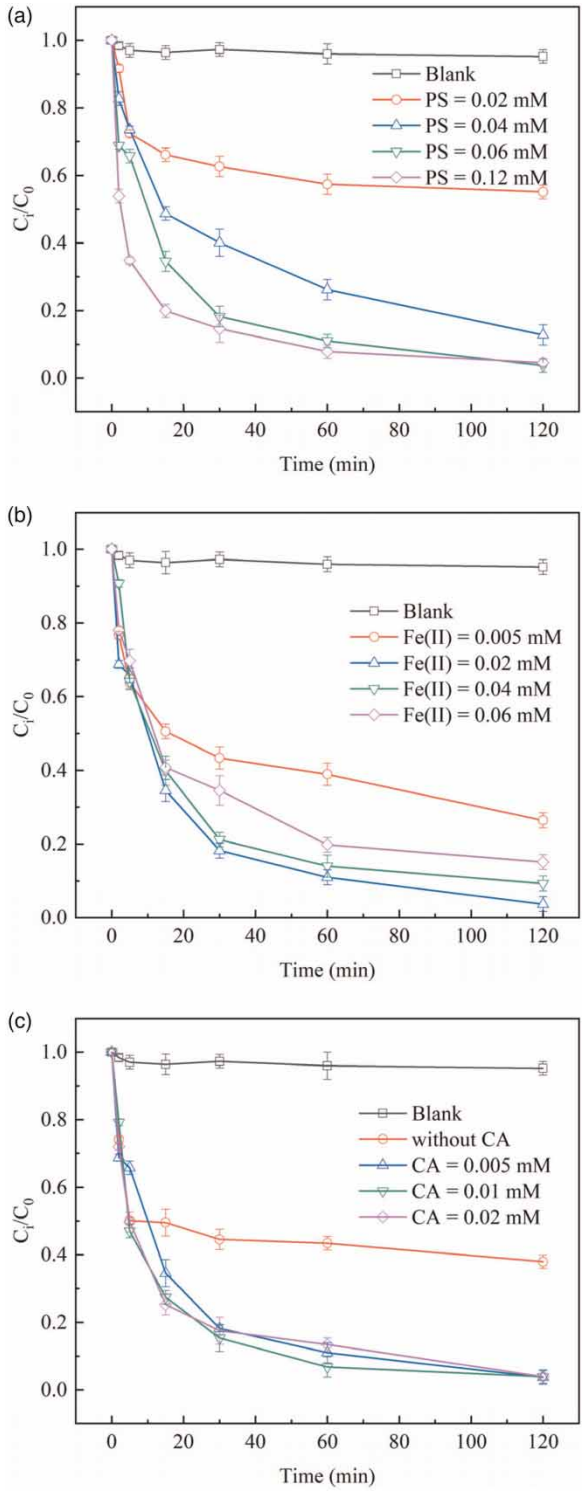

Figure 3 | Effect of (a) PS dosage ($[Fe(II)]_0 = 0.02$ mM, $[CA]_0 = 0.005$ mM, $[FLT]_0 = 0.001$ mM), (b) Fe(II) dosage ($[PS]_0 = 0.06$ mM, $[CA]_0 = 0.005$ mM, $[FLT]_0 = 0.001$ mM), and (c) CA dosage ($[PS]_0 = 0.06$ mM, $[Fe(II)]_0 = 0.02$ mM, $[FLT]_0 = 0.001$ mM) on FLT degradation.

loss, and for another thing, excessive CA could form a very stable chelate with Fe(II), which was not conducive to the catalytic reaction of Fe(II) (Rastogi *et al.* 2009b). k and $t_{1/2}$ did not change significantly when CA was increased from 0.005 to 0.01 mM, so the CA dosage was determined to be 0.005 mM considering the remediation cost. Therefore, in the following experiments, the doses of PS, Fe(II), CA and initial FLT concentration were set as 0.06, 0.02, 0.005 and 0.001 mM, respectively.

3.3. Effect of groundwater matrixes on FLT degradation

3.3.1. Effect of initial pH on FLT degradation

It is well known that the initial pH of the solution has a significant effect on ROS generation, thus the initial solution pH (3, 5, 7, 9 and 11) was adjusted by 0.1 M H_2SO_4 or 0.1 M NaOH to explore the effect of initial solution pH in the PS/Fe(II)/CA system and the results are shown in Figure 4(a) and Table 3. FLT removal reached 99.4 and 95.1% only at the initial pH of 3 and 5, while FLT removal plummeted to 19.1, 6.2 and 5.7% when the initial pH was increased to 7, 9 and 11,

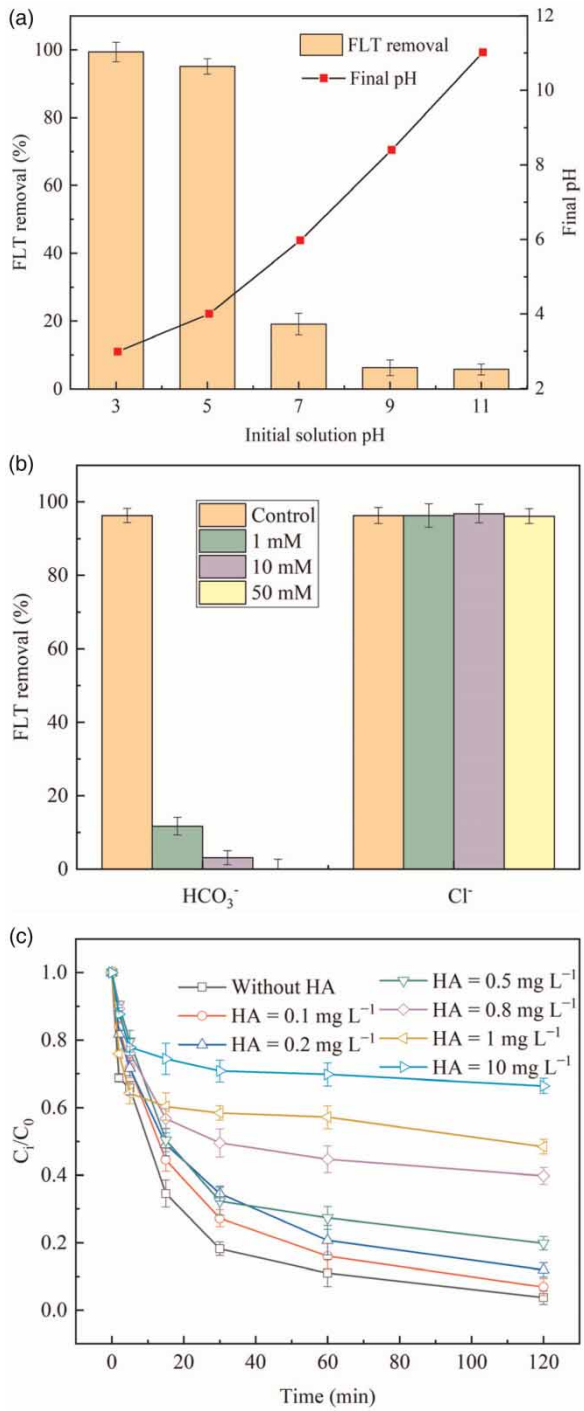

Figure 4 | Effects of (a) initial solution pH, (b) anions (Cl^- and HCO_3^-) and (c) HA on FLT degradation in PS/Fe(II)/CA system. $[PS]_0 = 0.06$ mM, $[Fe\ (II)]_0 = 0.02$ mM, $[CA]_0 = 0.005$ mM, $[FLT]_0 = 0.001$ mM.

Table 3 | Parameter values in PS/Fe(II)/CA system in groundwater matrixes

Experimental conditions	PS/Fe(II)/CA/FLT	pH (initial/final)	FLT removal (%)
pH = 3.0	60/20/5/1	3.03/2.99	99.4
pH = 5.0		4.98/4.00	95.1
pH = 7.0		7.02/5.97	19.1
pH = 9.0		8.99/8.40	6.3
pH = 11.0		10.96/11.02	5.7
Cl^- = 1 mM	60/20/5/1	4.69/3.98	96.3
Cl^- = 10 mM		4.68/4.12	96.8
Cl^- = 50 mM		4.86/5.97	96.1
HCO_3^- = 1 mM		6.47/7.91	11.7
HCO_3^- = 10 mM		8.30/8.42	3.1
HCO_3^- = 50 mM		8.41/8.37	0
HA = 0.1 mg L^{-1}	60/20/5/1	4.36/3.84	93.1
HA = 0.2 mg L^{-1}		4.53/4.12	88.1
HA = 0.5 mg L^{-1}		4.56/4.09	80.2
HA = 0.8 mg L^{-1}		4.50/4.12	60.2
HA = 1 mg L^{-1}		4.58/3.93	51.6
HA = 10 mg L^{-1}		4.72/4.04	33.6

respectively, indicating that this system could only effectively degrade FLT in a limited acidic pH range. This result was ascribed in detail for the following reasons. First of all, as the solution pH increased, Fe(II)-CA chelation was converted to Fe(II)-(OH)-CA and Fe(II)-$(OH)_2$-CA, which were more stable and difficult to release Fe(II) into the solution, thereby inhibiting the activation of PS (Kusic *et al.* 2011). Then, a high solution pH led to the low solubility of free Fe(II) and promoted the precipitation of $Fe(OH)_2$ and $Fe(OH)_3$, thus reducing the production of ROS (Han *et al.* 2015). What is more, $SO_4^{-\bullet}$ would convert to $HO^\bullet$ under alkaline conditions (Equation (10)), leading to more generation of $HO^\bullet$. However, SO_4^{2-}, as one of the inevitable products of PS, would slightly inhibit the activity of $HO^\bullet$ to some extent (Liang *et al.* 2007). In conclusion, compared to neutral or basic conditions, the acidic condition was more favorable for FLT removal by the PS/Fe(II)/CA system:

$$SO_4^{-\bullet} + OH^- \rightarrow HO^\bullet + SO_4^{2-} + H^+ \quad (10)$$

3.3.2. Effect of anions on FLT degradation

To further study the application of the PS/Fe(II)/CA system in practical scenarios, Figure 4(b) and Table 3 show the effect of two common anions in groundwater, HCO_3^- and Cl^-, on FLT degradation. To investigate the behavior of various concentrations of anion in this system, 1, 10 and 50 mM were set for each anion. The inhibitory effect was observed in the presence of all various concentrations of HCO_3^-, and FLT removal was decreased from 96.3 to 11.7, 3.1 and 0% when increasing the concentration of HCO_3^- from 0 to 1, 10 and 50 mM, respectively, mainly because HCO_3^- would consume $HO^\bullet$ and $SO_4^{-\bullet}$ (Equations (11) and (12)). Besides, the presence of HCO_3^- could act as a buffer to prevent drastic changes in solution pH, thus impairing FLT degradation (Dong *et al.* 2019):

$$HCO_3^- + HO^\bullet \rightarrow OH^- + HCO_3^\bullet \quad (11)$$

$$HCO_3^- + SO_4^{-\bullet} \rightarrow SO_4^{2-} + HCO_3^\bullet \quad (12)$$

The presence of Cl^- may affect FLT degradation in a negative way by complexing with Fe(II) and Fe(III) to form

chloro-iron complexes (Equations (13)–(15)), and interacting with $HO^{\bullet}$ forming less reactive species, such as $Cl_2^{-\bullet}$ and $SO_4^{-\bullet}$ (Equations (16)–(19)):

$$Fe(II) + Cl^- \rightarrow FeCl^+ \quad (13)$$

$$Fe(III) + Cl^- \rightarrow FeCl^{2+} \quad (14)$$

$$Fe(III) + 2C1^- \rightarrow FeC1_2^+ \quad (15)$$

$$Cl^- + HO^{\bullet} \rightarrow ClHO^{-\bullet} k = 4.3 \times 10^9 M^{-1}s^{-1} \quad (16)$$

$$ClHO^{-\bullet} + H^+ \rightarrow Cl^{\bullet} + H_2O \; k = 10^9 M^{-1}s^{-1} \quad (17)$$

$$Cl^- + Cl^{\bullet} \rightarrow Cl_2^{-\bullet} \quad (18)$$

$$SO_4^{2-} + HO^{\bullet} \rightarrow OH^- + SO_4^{-\bullet} \quad (19)$$

In the presence of Cl^-, this system degraded at least 96% FLT within the concentration range surveyed in this study, which was not consistent with the recognized results raised above. It was concluded that although Cl^- was a scavenger of free radicals, more $SO_4^{-\bullet}$ and $HO^{\bullet}$ were generated through complex free radical chain reactions to improve FLT removal. Monteagudo *et al.* (2015) found that although Cl^- could consume $HO^{\bullet}$, it could also continue to produce more $HO^{\bullet}$ through the reaction Equations (20)–(22). Wang & Wang (2020) also discovered that the hypochlorous acid radicals formed from Equation (16) could be quickly converted to $HO^{\bullet}$ through Equation (23), indicating that there was less or no loss of $HO^{\bullet}$ and therefore no inhibition for FLT removal. In addition, the concentration of Cl^- may be several orders of magnitude higher than the concentration of $HO^{\bullet}$ due to the limited oxidant dose (Lian *et al.* 2017), which remedies the lower reaction between $Cl^{\bullet}$ and FLT:

$$Cl^{\bullet} + H_2O \rightarrow \; HO^{\bullet} + HCl \quad (20)$$

$$Cl_2^{-\bullet} + H_2O \rightarrow \; HO^{\bullet} + 2Cl^- + H^+ \quad (21)$$

$$Cl_2^{-\bullet} + OH^- \rightarrow HO^{\bullet} \; + 2Cl^- \quad (22)$$

$$ClHO^{-\bullet} \rightarrow Cl^- + HO^{\bullet} \quad (23)$$

Hu *et al.* (2019) reported that the representative anions, including sulfate and nitrate, had negligible effect on *p*-Nitrophenol removal in the persulfate/microwave heating system, and Diao *et al.* (2020) had the similar finding that no significant effect of sulfate as well as nitrate on bisphenol A degradation in a heterogeneous ultrasound-enhanced sludge biochar catalyst/persulfate process. In addition, the dose of PS was only set at 0.06 mM in this experiment, so the sulfate produced by decomposition was small enough to affect FLT degradation.

3.3.3. Effect of humic acid on FLT degradation

Actual groundwater is abundant in natural organic matter (NOM), and Lin *et al.* (2017) found that the electron-rich groups in NOM can react with $SO_4^{-\bullet}$ and $HO^{\bullet}$. Since humic acid (HA) is an important component of NOM, it was selected as a representative of NOM to study its effect on FLT degradation in the PS/Fe(II)/CA system. Generally, the concentration of HA substances in groundwater varies from 1 to 50 mg L^{-1} (Li *et al.* 2019a, 2019b). Considering the limited chemical dosing in the experiment, the HA concentration range was set to 0.1–10 mg L^{-1}, and different concentrations were set in the range of 0.1–1 mg L^{-1} to carefully examine the effect of HA on the reaction. As shown in Figure 4(c), it is obvious that FLT degradation decreased with the increasing HA concentration, proving HA had a significant inhibitory effect on FLT degradation. On the one hand, as mentioned above, HA could consume $HO^{\bullet}$ and $SO_4^{-\bullet}$ and compete with FLT, resulting in a lower FLT removal. On the other hand, while HA competed for $SO_4^{-\bullet}$ and $HO^{\bullet}$, HA also inhibited the regeneration of Fe(II) (Wang & Lemley 2004), which led to the reduction of ROS and FLT degradation.

3.4. Mechanism of FLT degradation in the PS/Fe(II)/CA system

3.4.1. Identification of ROS in the PS/Fe(II)/CA system

According to other research reports (Yu *et al.* 2018), several ROS ($HO^{\bullet}$, $SO_4^{-\bullet}$ and $O_2^{-\bullet}$) are generated in a PS system activated by Fe(II), which may be produced in the PS/Fe(II)/CA process as well. Nitrobenzene (NB) as $HO^{\bullet}$ probe compound, anisole (AN) as both $HO^{\bullet}$ and $SO_4^{-\bullet}$ probe compound and carbon tetrachloride (CT) as $O_2^{-\bullet}$ probe compound to confirm the generated ROS in this process (see Supplementary material). As shown in Figure S3, all three probes were degraded to varying degrees and especially in the PS/Fe(II)/CA system, demonstrating the presence of $HO^{\bullet}$, $SO_4^{-\bullet}$, $O_2^{-\bullet}$, and the addition of CA could promote the generation of ROS. As far as we know, there was no suitable $^1O_2$ probe due to the insolubility of some potential chemicals in water and insensitivity to $^1O_2$ (Krasnovsky *et al.* 2008; Entradas *et al.* 2020). Therefore, EPR was used to determine whether there was $^1O_2$ during FLT oxidation in the PS/Fe(II)/CA system.

To further confirm the presence of ROS, EPR detection was used in this study. As shown in Figure 5, DMPO-OH adducts, DMPO-SO_4 adducts and TEMP-$^1O_2$ adducts were found in the PS/Fe(II)/CA system, indicating the presence of $HO^{\bullet}$, $SO_4^{-\bullet}$ and $^1O_2$. However, probably due to the low concentration and instability of $O_2^{-\bullet}$, no peaks were observed for the adducts composed of DMPO and $O_2^{-\bullet}$ (Fang *et al.* 2013).

Isopropanol (IPA) acted as a scavenger for $HO^{\bullet}$ and $SO_4^{-\bullet}$, furfuryl alcohol (FFA) acted as a scavenger for $HO^{\bullet}$ and $^1O_2$, while at the same time TBA and chloroform (CF) acted as scavengers for $HO^{\bullet}$ and $O_2^{-\bullet}$, respectively (see Supplementary material). As shown in Figure 6, FLT could be degraded by 96.3% without scavengers, while FLT degradation drastically

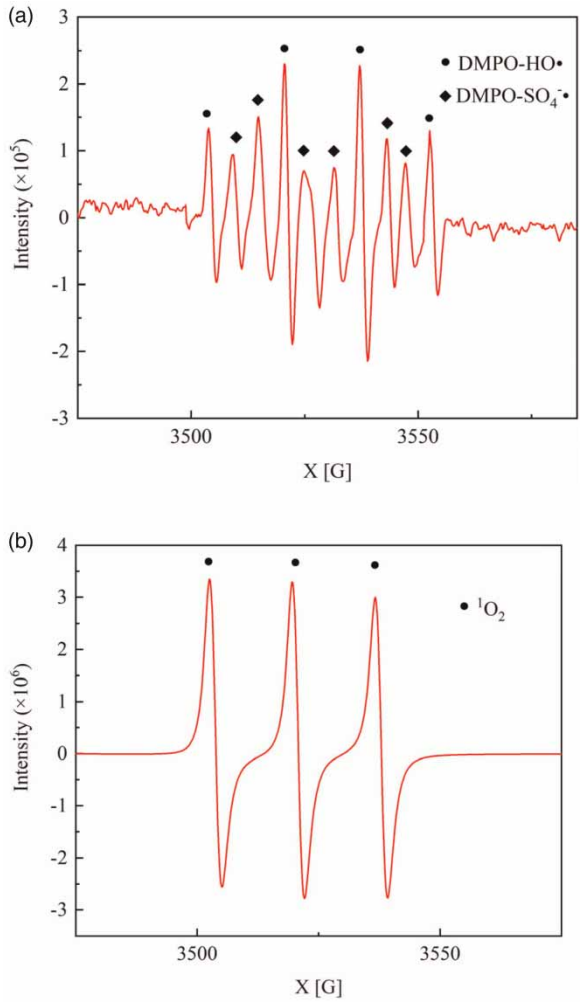

Figure 5 | EPR spectra at the reaction time of 10 min in the PS/Fe(II)/CA system, (a) DMPO as radical trap and (b) TEMP as radical trap.

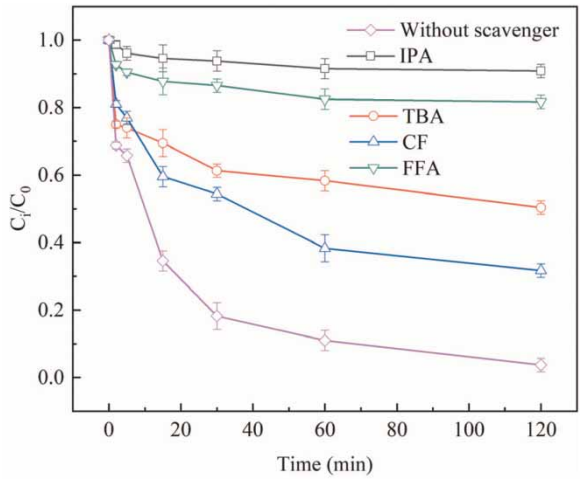

Figure 6 | Effect of scavengers on FLT degradation in the PS/Fe(II)/CA system. $[IPA]_0 = [TBA]_0 = [CF]_0 = [FFA]_0 = 10$ mM, $[PS]_0 = 0.06$ mM, $[Fe\ (II)]_0 = 0.02$ mM, $[CA]_0 = 0.005$ mM, $[FLT]_0 = 0.001$ mM.

dropped to 50.6% after the addition of TBA, which revealed that $HO^{\bullet}$ was the dominant ROS in FLT degradation. Besides, FLT degradation was also significantly inhibited after the excess IPA addition, indicating that FLT removal also depended on $SO_4^{-\bullet}$. Notably, 27.9% of FLT was held back with CF addition, demonstrating that a certain amount of $O_2^{-\bullet}$ was generated and made a non-negligible contribution to FLT degradation. Finally, FLT removal was decreased by 32.3% after FFA addition compared to the inhibition of TBA, which elucidated that $^1O_2$ also contributed significantly to FLT degradation. In summary, both $SO_4^{-\bullet}$ and $HO^{\bullet}$ were dominant ROS for FLT removal, along which $HO^{\bullet}$ performed a more important role in FLT degradation. This was mainly due to a large amount of $HO^{\bullet}$ being converted from $SO_4^{-\bullet}$ (Equation (10)).

3.4.2. Possible FLT degradation pathways

The intermediates of FLT degradation were detected by GC-MS, which are shown in Table S6. Several chromatograms of intermediates are supplied in Figure S4. Based on the degradation products, the following possible degradation pathway was proposed (Figure 7). First, FLT was decomposed into *o*-dimethylbenzene (*o*-xylene) and naphthalene after being attacked by ROS (the attack position is shown by the arrow). Second, $HO^{\bullet}$ attacked naphthalene and made naphthalene undergo hydroxylation to form 1,4-naphthol (Onwudili & Williams 2007), which in turn formed 1,4-naphthoquinone under continued attack by $HO^{\bullet}$ (Bunce *et al.* 1997). After 1,4-naphthoquinone was produced from hydroxylation, it formed phthalic anhydride

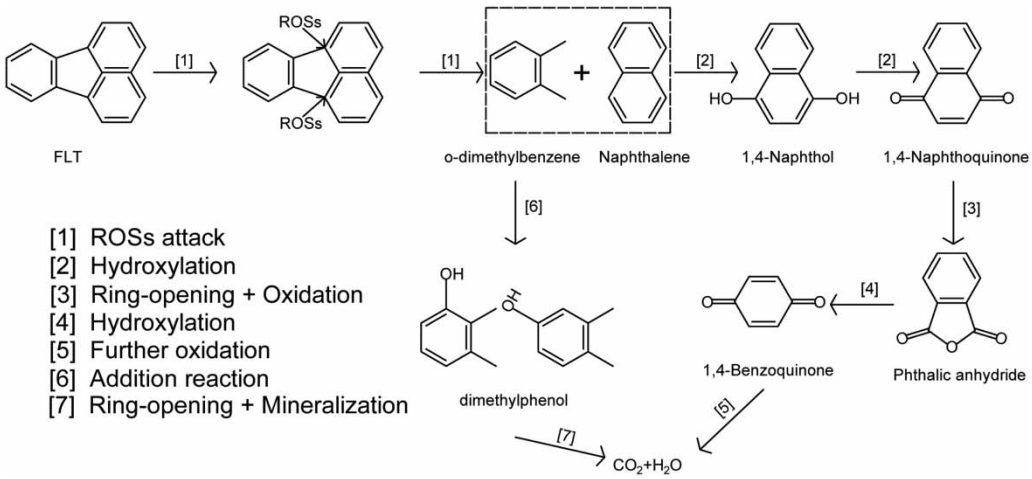

Figure 7 | Proposed FLT degradation pathways in PS/Fe(II)/CA system. $[PS]_0 = 0.06$ mM, $[Fe\ (II)]_0 = 0.02$ mM, $[CA]_0 = 0.005$ mM, $[FLT]_0 = 0.001$ mM.

by ring-opening, which generated 1,4-benzoquinone through hydroxylation successively (Gu *et al.* 2018). In addition, the benzene ring of *o*-xylene was attacked by $HO^{\bullet}$ to form two dimethylphenol isomers, which were subsequently decomposed into carbon dioxide and water by ring-opening and completely mineralization (Xue *et al.* 2018).

3.5. Effect of surfactants on FLT degradation

PAHs, including FLT, are commonly found in contaminated soil due to their low solubility in water and their high adsorption capacity to soil (Galiulin *et al.* 2002). Surfactants could act as solubilizers by reducing surface tension, which could desorb contaminants from the soil and transport them to the aqueous phase for further treatment (Lamichhane *et al.* 2017). However, some studies have shown that surfactants may affect the degradation of pollutants by advanced oxidation (Ying 2006). The effects of Tween 80 (TW-80), sodium dodecyl sulfate (SDS), polyoxyethylene octyl phenyl ether (TX-100) and polyoxyethylene lauryl ether (Brij-35) on FLT removal in PS/Fe(II)/CA system were investigated and their properties are listed in Table S2. The surfactant concentrations in actual contaminated site remediation are generally from 1.0 to 10 g L^{-1} (Besha *et al.* 2018), and the concentration was set as 1.0 g L^{-1}, considering the limited dose applied in this system.

As shown in Figure 8, both k and FLT degradation showed a significant decrease after the addition of surfactants, which proved that surfactants could inhibit FLT removal in this system. For one thing, surfactant, as an organic compound that could be decomposed by oxidation, would compete with FLT for ROS (Mousset *et al.* 2014). Sun *et al.* (2021) found that TW-80, Brij-35 and TX-100 could inhibit trichloroethene (TCE) degradation by competing with TCE to consume $HO^{\bullet}$ through EPR experiments. For another thing, when the surfactant concentration was greater than 1.0 critical micelle concentrations (CMC), the surfactant would exist as micelles, which consist of the hydrophobic core and hydrophilic shell, and with regard to hydrophobic FLT molecule, it would tend to be stuck in the micelle core (Trellu *et al.* 2017). In the case of FLT

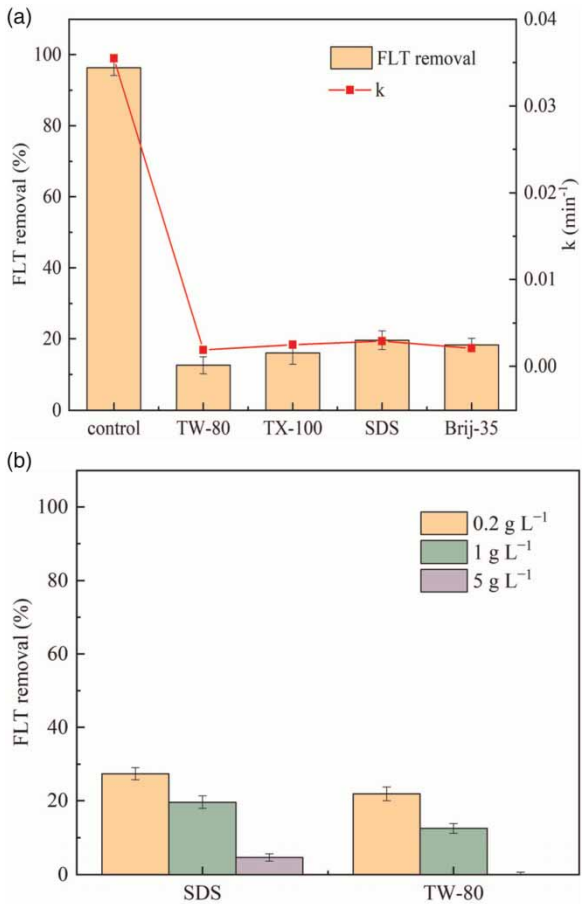

Figure 8 | Effect of (a) different surfactants ($[TW\text{-}80]_0 = [SDS]_0 = [TX\text{-}100]_0 = [Brij\text{-}35]_0 = 1$ g L^{-1}), and (b) TW-80 and SDS concentrations on FLT degradation in the PS/Fe(II)/CA system. $[PS]_0 = 0.06$ mM, $[Fe\ (II)]_0 = 0.02$ mM, $[CA]_0 = 0.005$ mM, $[FLT]_0 = 0.001$ mM.

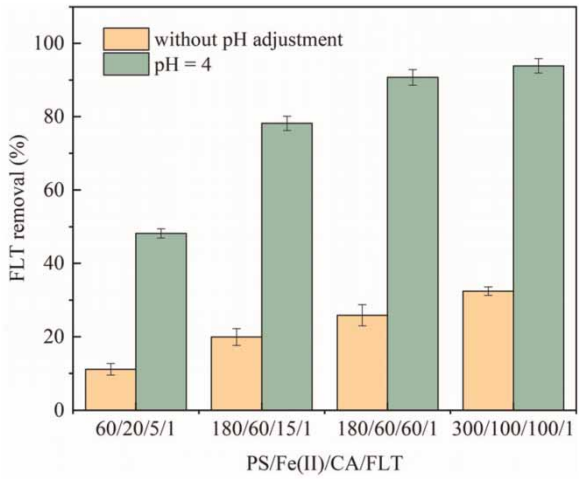

Figure 9 | FLT degradation performance in actual groundwater in the PS/Fe(II)/CA system. $[FLT]_0 = 0.001$ mM.

molecules trapped in the micelle core, ROS need to attack the micelle and open it before they could degrade FLT. In addition, the effects on various concentrations of TW-80 and SDS, which are representatives of popular nonionic and anionic surfactants, were also investigated on FLT degradation. It is worth noting that the inhibition effect of TW-80 was slightly stronger than SDS at the same concentration, probably because the CMC of TW-80 is much smaller than SDS, so it could create more micelles in the solution thus requiring more ROS to open it.

3.6. Removal of FLT in actual groundwater remediation

To investigate the applicability of the PS/Fe(II)/CA system for FLT degradation, experiments were conducted with actual groundwater instead of ultrapure water. The major characteristics of the actual groundwater are displayed in Table S5. As shown in Figure 9, when the molar ratio of PS/Fe(II)/CA/FLT was 60/20/5/1, FLT removal was only 11.1% in 120 min. The significant decrease in degradation was mainly due to the adverse effects of the high actual groundwater pH and the high concentration of HCO_3^-. The effect of higher agent doses on FLT degradation was investigated and the results were less than satisfactory. Therefore, the initial solution pH was adjusted to 4 using 0.1 M H_2SO_4, and a significant increase of FLT degradation was unexpectedly acquired. At pH = 4, FLT degradation reached 90.7 and 93.9% at 180/60/60/1 and 300/100/100/1 molar ratio of PS/Fe(II)/CA/FLT (Table 2), respectively, mainly because H^+ eliminated the inhibitory effect of HCO_3^- by reacting with it under acidic conditions. Considering that the pH of the solution after the reaction were all below 4, natural alkaline substances such as lime could be added to the restored groundwater (Long *et al.* 2014). Clearly, adjusting the initial solution pH after an appropriate increment of chemical dosage was a feasible way to remediate FLT in groundwater.

4. CONCLUSIONS

In this research, 96.3% FLT removal was achieved in 120 min when the PS/Fe(II)/CA/FLT molar ratio was 60/20/5/1 and the % RSE in PS/Fe(II)/CA/FLT was 2.9%. Compared with the PS/Fe(II) system, the addition of CA could dramatically improve FLT degradation performance by chelating Fe(II)/Fe(III) and producing more ROS. The solution pH had a strong influence on the PS/Fe(II)/CA system, and the acidic condition was favorable for FLT removal. HCO_3^- and HA had a certain inhibition on FLT degradation, which became obvious as the concentrations increased, but Cl^- had almost no effect on FLT degradation. The results of probe tests, EPR detection and scavenging experiments indicated that $HO^\bullet$ and $SO_4^{-\bullet}$ acted predominantly on FLT degradation. The possible FLT degradation pathway was proposed based on the detection of *o*-xylene and naphthalene during FLT degradation by GC-MS. The FLT molecule was attacked by ROS to split into *o*-xylene and naphthalene, where naphthalene and *o*-xylene eventually formed CO_2 and H_2O through hydroxylation, ring-opening, oxidation and addition reactions, ring-opening, and mineralization, respectively. The presence of surfactants inhibited FLT degradation and the inhibition was slightly pronounced for surfactants with low CMC at the same concentration.

Experiments conducted in actual groundwater indicated that the PS/Fe(II)/CA system could be used to remediate FLT in actual groundwater.

ACKNOWLEDGEMENTS NSFC

This study was financially supported by a grant from the National Natural Science Foundation of China (No. 41977164).

CONFLICTS OF INTERESTS

The authors declare that they have no known competing financial interests or personal relationships that could have appeared to influence the work reported in this paper.

DATA AVAILABILITY STATEMENT

All relevant data are included in the paper or its Supplementary Information.

REFERENCES

Ayoub, G. & Ghauch, A. 2014 Assessment of bimetallic and trimetallic iron-based systems for persulfate activation: application to sulfamethoxazole degradation. *Chemical Engineering Journal* **256**, 280–292.

Baalbaki, A., Eddine, N. Z., Jaber, S., Amasha, M. & Ghauch, A. 2018 Rapid quantification of persulfate in aqueous systems using a modified HPLC unit. *Talanta* **178**, 237–245.

Baciocchi, R. 2013 Principles, developments and design criteria of in situ chemical oxidation. *Water, Air, & Soil Pollution* **224** (12), 1–11.

Besha, A. T., Bekele, D. N., Naidu, R. & Chadalavada, S. 2018 Recent advances in surfactant-enhanced In-Situ chemical oxidation for the remediation of non-aqueous phase liquid contaminated soils and aquifers. *Environmental Technology & Innovation* **9**, 303–322.

Bunce, N. J., Liu, L., Zhu, J. & Lane, D. A. 1997 Reaction of naphthalene and its derivatives with hydroxyl radicals in the gas phase. *Environmental Science & Technology* **31** (8), 2252–2259.

Diao, Z. H., Dong, F. X., Yan, L., Chen, Z. L., Qian, W., Kong, L. J., Zhang, Z. W., Zhang, T., Tao, X. Q., Du, J. J., Jiang, D. & Chu, W. 2020 Synergistic oxidation of Bisphenol A in a heterogeneous ultrasound-enhanced sludge biochar catalyst/persulfate process: reactivity and mechanism. *Journal of Hazardous Materials* **384**, 121385.

Dong, H., Wang, B., Li, L., Wang, Y., Ning, Q., Tian, R., Li, R., Chen, J. & Xie, Q. 2019 Activation of persulfate and hydrogen peroxide by using sulfide-modified nanoscale zero-valent iron for oxidative degradation of sulfamethazine: a comparative study. *Separation and Purification Technology* **218**, 113–119.

El Asmar, R., Baalbaki, A., Abou Khalil, Z., Naim, S., Bejjani, A. & Ghauch, A. 2021 Iron-based metal organic framework MIL-88-A for the degradation of naproxen in water through persulfate activation. *Chemical Engineering Journal* **405**, 126701.

Entradas, T., Waldron, S. & Volk, M. 2020 The detection sensitivity of commonly used singlet oxygen probes in aqueous environments. *Journal of Photochemistry and Photobiology. B, Biology* **204**, 111787.

Fang, G. D., Dionysiou, D. D., Al-Abed, S. R. & Zhou, D. M. 2013 Superoxide radical driving the activation of persulfate by magnetite nanoparticles: implications for the degradation of PCBs. *Applied Catalysis B Environmental* **129**, 325–332.

Fang, L., Liu, K., Li, F., Zeng, W., Hong, Z., Xu, L., Shi, Q. & Ma, Y. 2021 New insights into stoichiometric efficiency and synergistic mechanism of persulfate activation by zero-valent bimetal (Iron/Copper) for organic pollutant degradation. *Journal of Hazardous Materials* **403**, 123669.

Galiulin, R. V., Bashkin, V. N. & Galiulina, R. A. 2002 Behavior of persistent organic pollutants in the air-plant-soil system. *Water, Air, and Soil Pollution* **137** (1), 179–191.

Gan, S. & Ng, H. K. 2012 Inorganic chelated modified-Fenton treatment of polycyclic aromatic hydrocarbon (PAH)-contaminated soils. *Chemical Engineering Journal* **180**, 1–8.

Ghauch, A., Ayoub, G. & Naim, S. 2013 Degradation of sulfamethoxazole by persulfate assisted micrometric Fe_0 in aqueous solution. *Chemical Engineering Journal* **228**, 1168–1181.

Ghauch, A., Baydoun, H. & Dermesropian, P. 2011 Degradation of aqueous carbamazepine in ultrasonic/Fe0/H_2O_2 systems. *Chemical Engineering Journal* **172** (1), 18–27.

Ghauch, A., Tuqan, A. M. & Kibbi, N. 2015 Naproxen abatement by thermally activated persulfate in aqueous systems. *Chemical Engineering Journal* **279**, 861–873.

Ghauch, A., Baalbaki, A., Amasha, M., El Asmar, R. & Tantawi, O. 2017 Contribution of persulfate in UV-254 nm activated systems for complete degradation of chloramphenicol antibiotic in water. *Chemical Engineering Journal* **317**, 1012–1025.

Gu, M., Sui, Q., Farooq, U., Zhang, X., Qiu, Z. & Lyu, S. 2018 Degradation of phenanthrene in sulfate radical based oxidative environment by nZVI-PDA functionalized rGO catalyst. *Chemical Engineering Journal* **354**, 541–552.

Gupta, S. S. & Gupta, Y. K. 1981 Hydrogen ion dependence of the oxidation of iron (II) with peroxydisulfate in acid perchlorate solutions. *Inorganic Chemistry* **20** (2), 454–457.

Han, D., Wan, J., Ma, Y., Wang, Y., Li, Y., Li, D. & Guan, Z. 2015 New insights into the role of organic chelating agents in Fe (II) activated persulfate processes. *Chemical Engineering Journal* **269**, 425–433.

Harvey Jr., A. E., Smart, J. A. & Amis, E. S. 1955 Simultaneous spectrophotometric determination of iron (II) and total iron with 1, 10-phenanthroline. *Analytical Chemistry* **27** (1), 26–29.

Hu, L., Zhang, G., Wang, Q., Wang, X. & Wang, P. 2019 Effect of microwave heating on persulfate activation for rapid degradation and mineralization of p-nitrophenol. *ACS Sustainable Chemistry & Engineering* **7** (13), 11662–11671.

Kadri, T., Rouissi, T., Brar, S. K., Cledon, M., Sarma, S. & Verma, M. 2017 Biodegradation of polycyclic aromatic hydrocarbons (PAHs) by fungal enzymes: a review. *Journal of Environmental Sciences* **51**, 52–74.

Keyte, I. J., Harrison, R. M. & Lammel, G. 2013 Chemical reactivity and long-range transport potential of polycyclic aromatic hydrocarbons – a review. *Chemical Society Reviews* **42** (24), 9333–9391.

Krasnovsky Jr., A. A., Roumbal, Y. V. & Strizhakov, A. A. 2008 Rates of 1O2 (1Δg) production upon direct excitation of molecular oxygen by 1270 nm laser radiation in air-saturated alcohols and micellar aqueous dispersions. *Chemical Physics Letters* **458** (1–3), 195–199.

Kusic, H., Peternel, I., Ukic, S., Koprivanac, N., Bolanca, T., Papic, S. & Bozic, A. L. 2011 Modeling of iron activated persulfate oxidation treating reactive azo dye in water matrix. *Chemical Engineering Journal* **172** (1), 109–121.

Lamichhane, S., Krishna, K. B. & Sarukkalige, R. 2017 Surfactant-enhanced remediation of polycyclic aromatic hydrocarbons: a review. *Journal of Environmental Management* **199**, 46–61.

Li, L., Lai, C., Huang, F., Cheng, M., Zeng, G., Huang, D., Li, B., Liu, S., Zhang, M. M. & Qin, L. 2019a Degradation of naphthalene with magnetic bio-char activate hydrogen peroxide: synergism of bio-char and Fe–Mn binary oxides. *Water Research* **160**, 238–248.

Li, X., Wu, B., Zhang, Q., Xu, D., Liu, Y., Ma, F., Gu, Q. & Li, F. 2019b Mechanisms on the impacts of humic acids on persulfate/Fe^{2+}-based groundwater remediation. *Chemical Engineering Journal* **378**, 122142.

Lian, L., Yao, B., Hou, S., Fang, J., Yan, S. & Song, W. 2017 Kinetic study of hydroxyl and sulfate radical-mediated oxidation of pharmaceuticals in wastewater effluents. *Environmental Science & Technology* **51** (5), 2954–2962.

Liang, C., Bruell, C. J., Marley, M. C. & Sperry, K. L. 2004 Persulfate oxidation for in situ remediation of tce. ii. activated by chelated ferrous ion. *Chemosphere* **55** (9), 1225–1233.

Liang, C., Wang, Z. S. & Bruell, C. J. 2007 Influence of pH on persulfate oxidation of TCE at ambient temperatures. *Chemosphere* **66** (1), 106–113.

Liang, C., Huang, C. F., Mohanty, N. & Kurakalva, R. M. 2008 A rapid spectrophotometric determination of persulfate anion in ISCO. *Chemosphere* **73** (9), 1540–1543.

Liang, C., Liang, C. P. & Chen, C. C. 2009 Ph dependence of persulfate activation by EDTA/Fe (III) for degradation of trichloroethylene. *Journal of Contaminant Hydrology* **106** (3–4), 173–182.

Lin, Z. R., Zhao, L. & Dong, Y. H. 2017 Effects of low molecular weight organic acids and fulvic acid on 2,4,4'-trichlorobiphenyl degradation and hydroxyl radical formation in a goethite-catalyzed fenton-like reaction. *Chemical Engineering Journal* **326**, 201–209.

Lindsey, M. E. & Tarr, M. A. 2000 Quantitation of hydroxyl radical during Fenton oxidation following a single addition of iron and peroxide. *Chemosphere* **41** (3), 409–417.

Long, A., Lei, Y. & Zhang, H. 2014 In situ chemical oxidation of organic contaminated soil and groundwater using activated persulfate process. *Progress in Chemistry* **26** (05), 898.

Monteagudo, J. M., Durán, A., González, R. & Expósito, A. J. 2015 In situ chemical oxidation of carbamazepine solutions using persulfate simultaneously activated by heat energy, UV light, Fe^{2+} ions, and H_2O_2. *Applied Catalysis B Environmental* **176**, 120–129.

Mousset, E., Oturan, N., van Hullebusch, E. D., Guibaud, G., Esposito, G. & Oturan, M. A. 2014 Influence of solubilizing agents (cyclodextrin or surfactant) on phenanthrene degradation by electro-Fenton process–study of soil washing recycling possibilities and environmental impact. *Water Research* **48**, 306–316.

Naim, S. & Ghauch, A. 2016 Ranitidine abatement in chemically activated persulfate systems: assessment of industrial iron waste for sustainable applications. *Chemical Engineering Journal* **288**, 276–288.

Ogbuagu, D. H., Okoli, C. G., Gilbert, C. L. & Madu, S. 2011 Determination of the contamination of groundwater sources in Okrika Mainland with Polynuclear Aromatic Hydrocarbons (PAHs). *British Journal of Environment and Climate Change* **1** (3), 90.

Onwudili, J. A. & Williams, P. T. 2007 Reaction mechanisms for the decomposition of phenanthrene and naphthalene under hydrothermal conditions. *The Journal of Supercritical Fluids* **39** (3), 399–408.

Peluffo, M., Pardo, F., Santos, A. & Romero, A. 2016 Use of different kinds of persulfate activation with iron for the remediation of a PAH-contaminated soil. *Science of the Total Environment* **563**, 649–656.

Qian, Y., Zhang, J., Zhang, Y., Chen, J. & Zhou, X. 2016 Degradation of 2,4-dichlorophenol by nanoscale calcium peroxide: implication for groundwater remediation. *Separation and Purification Technology* **166**, 222–229.

Rastogi, A., Al-Abed, S. R. & Dionysiou, D. D. 2009a Effect of inorganic, synthetic and naturally occurring chelating agents on Fe (II) mediated advanced oxidation of chlorophenols. *Water Research* **43** (3), 684–694.

Rastogi, A., Al-Abed, S. R. & Dionysiou, D. D. 2009b Sulfate radical-based ferrous–peroxymonosulfate oxidative system for PCBs degradation in aqueous and sediment systems. *Applied Catalysis B Environmental* **85** (3–4), 171–179.

Sun, Y., Li, M., Gu, X., Danish, M., Shan, A., Ali, M., Qiu, Z., Sui, Q. & Lyu, S. 2021 Mechanism of surfactant in trichloroethene degradation in aqueous solution by sodium persulfate activated with chelated-Fe (II). *Journal of Hazardous Materials* **407**, 124814.

Tantawi, O., Baalbaki, A., El Asmar, R. & Ghauch, A. 2019 A rapid and economical method for the quantification of hydrogen peroxide (H_2O_2) using a modified HPLC apparatus. *Science of The Total Environment* **654**, 107–117.

Trellu, C., Oturan, N., Pechaud, Y., van Hullebusch, E. D., Esposito, G. & Oturan, M. A. 2017 Anodic oxidation of surfactants and organic compounds entrapped in micelles–Selective degradation mechanisms and soil washing solution reuse. *Water Research* **118**, 1–11.

Wang, Q. & Lemley, A. T. 2004 Kinetic effect of humic acid on alachlor degradation by anodic Fenton treatment. *Journal of Environmental Quality* **33** (6), 2343–2352.

Wang, J. & Wang, S. 2018 Activation of persulfate (PS) and peroxymonosulfate (PMS) and application for the degradation of emerging contaminants. *Chemical Engineering Journal* **334**, 1502–1517.

Wang, J. & Wang, S. 2020 Reactive species in advanced oxidation processes: formation, identification and reaction A. *Chemical Engineering Journal* **401**, 126158.

Wang, J., Zhang, X., Ling, W., Liu, R., Liu, J., Kang, F. & Gao, Y. 2017 Contamination and health risk assessment of PAHs in soils and crops in industrial areas of the Yangtze River Delta region, China. *Chemosphere* **168**, 976–987.

Wu, X., Gu, X., Lu, S., Xu, M., Zang, X., Miao, Z., Qiu, Z. & Qian, S. 2014 Degradation of trichloroethylene in aqueous solution by persulfate activated with citric acid chelated ferrous ion – sciencedirect. *Chemical Engineering Journal* **255** (255), 585–592.

Xue, Y., Lu, S., Fu, X., Sharma, V. K., Mendoza-Sanchez, I., Qiu, Z. & Sui, Q. 2018 Simultaneous removal of benzene, toluene, ethylbenzene and xylene (BTEX) by cao2 based Fenton system: enhanced degradation by chelating agents. *Chemical Engineering Journal* **331**, 255–264.

Yan, D. Y. & Lo, I. M. 2013 Removal effectiveness and mechanisms of naphthalene and heavy metals from artificially contaminated soil by iron chelate-activated persulfate. *Environmental Pollution* **178**, 15–22.

Ying, G. G. 2006 Fate, behavior and effects of surfactants and their degradation products in the environment. *Environment International* **32** (3), 417–431.

Yu, S., Gu, X., Lu, S., Xue, Y., Zhang, X., Xu, M., Qiu, Z. & Sui, Q. 2018 Degradation of phenanthrene in aqueous solution by a persulfate/percarbonate system activated with CA chelated-Fe (II). *Chemical Engineering Journal* **333**, 122–131.

Zhang, K., Zhou, X., Zhang, T., Yu, L., Qian, Z., Liao, W. & Li, C. 2017 Degradation of the earthy and musty odorant 2,4,6-tricholoroanisole by persulfate activated with iron of different valences. *Environmental Science & Pollution Research* **25** (4), 3435–3445.

First received 10 January 2022; accepted in revised form 25 April 2022. Available online 6 May 2022